

Colored TiO₂ hollow spheres for efficient water-splitting photocatalyst

Wanlu Cao ^a, Bo Wei ^b, Xianliang Fu ^c, Ning Ma^a, Hong Gao^a, Lingling Xu^a *

^a *Key Laboratory of Photonic and Electric Bandgap Materials, Ministry of Education, School of Physics and Electronic Engineering, Harbin Normal University, Harbin, 150025, China*

^b *Department of Physics, Harbin Institute of Technology, Harbin, 150080, China*

^c *College of Chemistry and Material Science, Huaibei Normal University, Huaibei, Anhui, 235000, China*

Electronic supplementary information (ESI):

SI-Experimental procedures

Preparation of Anatase TiO₂ Hollow Spheres

Anatase TiO₂ hollow spheres were synthesized through a solvothermal method,¹ and all the analytical grade chemical reagents were used without further purification. Firstly, oxalic acid dehydrate (1.92 g) was completely dissolved in isopropyl alcohol (80 mL) under magnetic stirring. Then 1 mL of tetrabutyl titanate was dropped into the solution with continuous stirring. The resulting yellowish solution was transferred into a 120 mL Teflon-lined stainless autoclave and heated at 180 °C for 2.5 h. After cooling down to the room temperature, the white precipitate was collected and washed with ethanol several times. As collected powder was dried at 60 °C for 12 h in vacuum to obtain the TiO₂ hollow sphere which was denoted as AHS.

Preparation of oxygen-deficient Anatase Hollow Spheres

In a typical preparation procedure, 0.5 g of TiO₂ hollow spheres and 0.33 g of NaBH₄ were mixed and grounded. Then the mixture was put into a 5 mL alumina crucible and then transferred into a tube furnace. The temperature of the furnace was programmed to rise at a constant heating rate of 5 °C/min to 300 °C and maintained for 20 min, 40min and 60min in N₂ atmosphere, respectively. After cooling down to room temperature, the oxygen-deficient anatase hollow sphere was obtained and the corresponding samples were named as AHS20, AHS40 and AHS60, respectively. Finally, the TiO₂ hollow sphere was collected and washed with ethanol and deionized water for several times followed by drying at 60 °C for 12 h in vacuum.

Sample characterizations

The crystal structure of the samples was investigated by using a Rigaku D/max-2600/PC X-ray diffractometer with CuK α radiation ($\lambda = 0.154178$ nm). The morphology of the samples was examined by a Hitachi SU-70 scanning electron microscope (SEM) and a FEI Tecai G2 F20 transmission electron microscopy (TEM, 200 kV accelerating voltage). The chemical and bonding environments were ascertained by using an X-ray photoelectron spectrometer (XPS, Thermofisher K-Alpha) with Al source. The standard binding energy of 284.60 eV from C 1s is selected as internal standard. Raman spectra were collected by using a LabRAM HR800 with an excitation wavelength of 488 nm. The electron paramagnetic resonance (EPR) was collected by using a JEOL JES FA200 spectrometer at 100 K. Surface areas were determined from nitrogen adsorption–desorption isotherms at liquid nitrogen temperature using a Quantachrome NOVA 2000e surface area analyzer. The Brunauer–Emmett–Teller (BET) method was used for the surface area calculation (1.42–3.13 m² g⁻¹).

Photocatalytic water splitting characterizations

The Pt cocatalyst was loaded by a photodeposition method.² The TiO₂ hollow sphere (0.1 g) was dispersed in 90 mL aqueous solution containing a desirable amount of H₂PtCl₆·6H₂O (0.1 mL, 10 mg·mL⁻¹) in a Pyrex glass reactor. 10 mL of methanol was then added to the suspension with magnetic stirring for 2 h in the dark. The photodeposition was carried out by illuminating the reactor using a 300 W Xenon lamp for 30 min with constant stirring. After the photoreaction, the precipitation was filtered and then dried 12 h at 60 °C in a vacuum oven.

H₂ production by photocatalytic water splitting was performed by using a closed circulation system (Perfect Light Company Labsolar-III) with a tightly closed reactor, which was kept at 25 °C for the whole reaction. A 300 W Xe lamp (Perfect Light Company Solaredge 700) was used as an artificial solar light source. Photocatalyst powder (100 mg) was dispersed in H₂O (90 mL) and methanol (30 mL) was added to the solution as a sacrificial reagent. The amount of H₂ generation was measured by using a gas chromatography (Techcomp GC 7900) with high-purity nitrogen as carrier gas.

To investigate the photoelectrochemical properties, the pristine and reduced TiO₂ films were prepared by dip-coating onto a 2×1.5 cm² fluorine-doped tin oxide (FTO) glass electrode. An exposed area of 1 cm² was illuminated and the remaining part of electrode was sealed by the insulating adhesive to reduce the current leakage. The PEC measurements were performed by an electrochemical workstation (Chenhua

CHI660E) using a three-electrode setup, in which the TiO₂ film on a FTO substrate, a Pt plate, and KCl-saturated calomel electrode were used as the working, counter, and reference electrode, respectively. 0.1 M Na₂SO₄ aqueous solution was used as the electrolyte (pH ≈ 7). A 300 W Xe lamp was used as the excitation source to simulate the sunlight irradiation. The potential was swept linearly at a scan rate of 10 mVs⁻¹ between -0.7 and 0.4 V_{SCE} in a 0.1 M Na₂SO₄ electrolyte (pH ≈ 7). The transient photocurrent responses were recorded in the dark and under illumination using the same electrochemical workstation. The Mott-Schottky plots were obtained from impedance-potential tests, which were conducted at a frequency of 1 KHz in the dark.

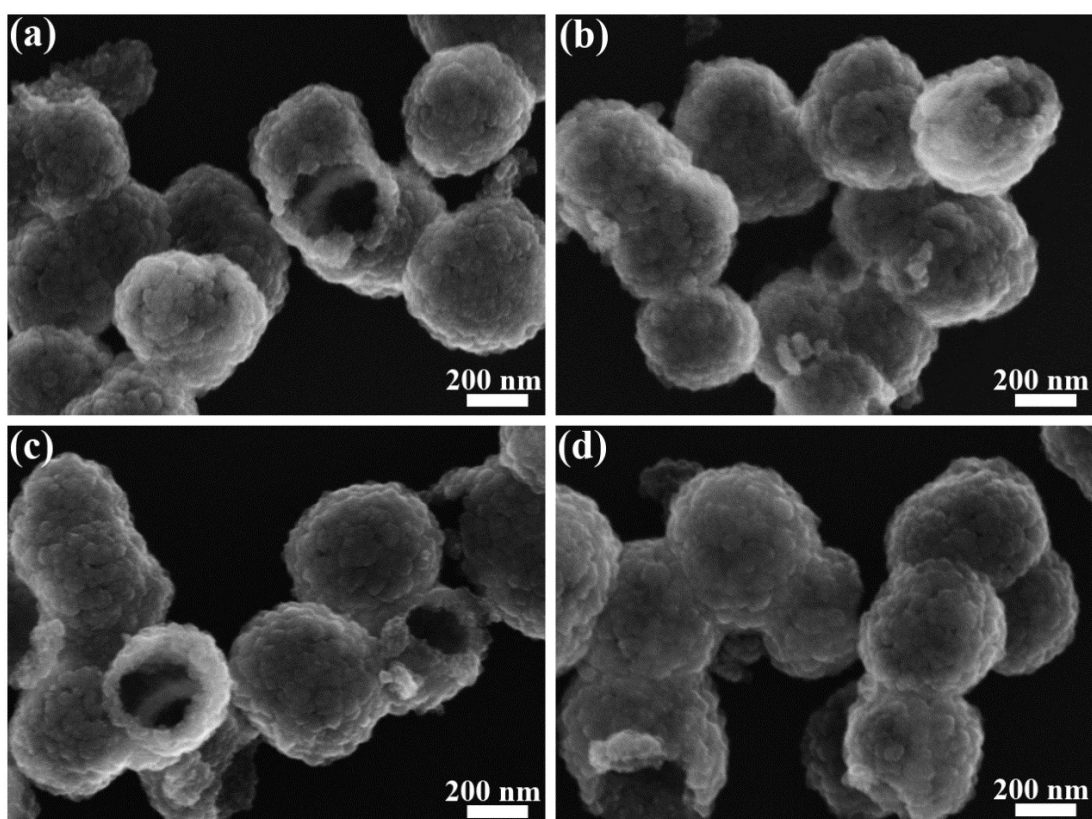


Fig. S1. SEM images of (a) AHS, (b) AHS20, (c) AHS40 and (d) AHS60.

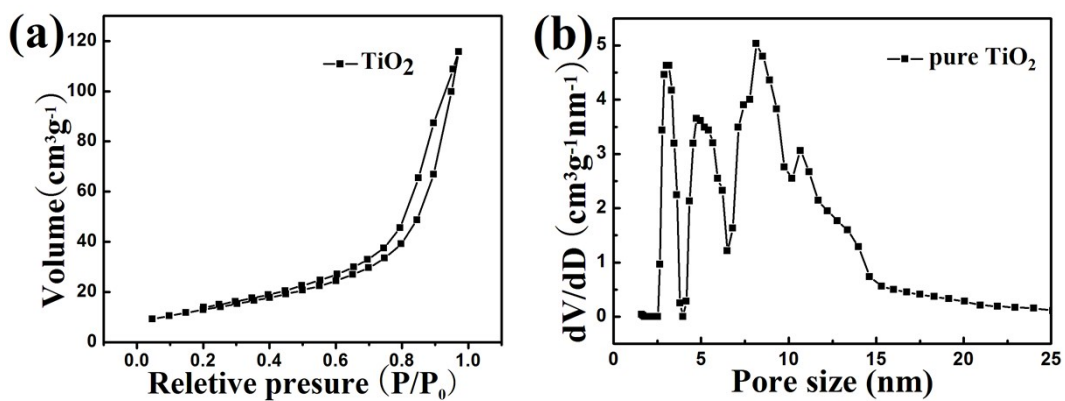
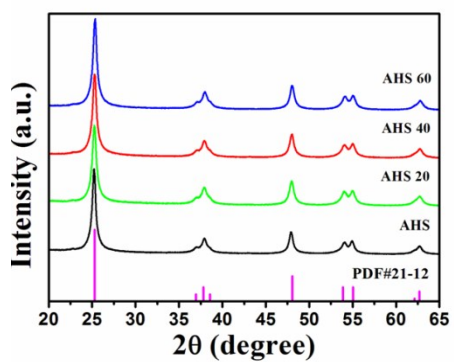


Fig. S2. (a) BET patterns of TiO₂ and (b) Pore size distribution of AHS.



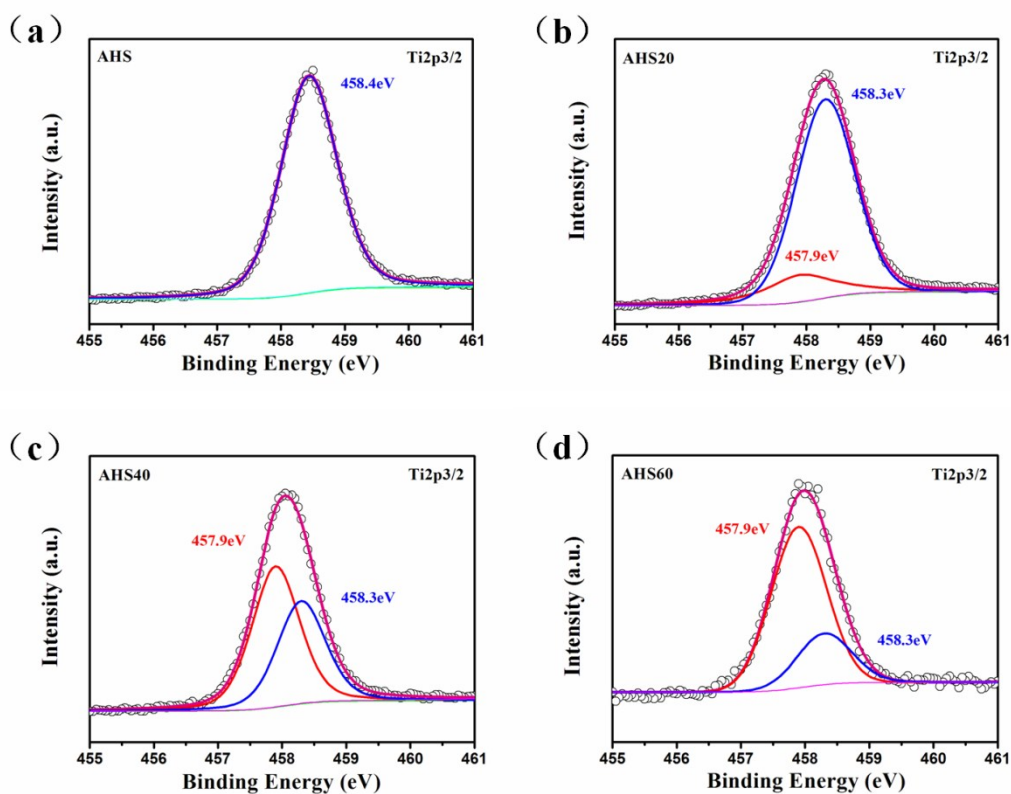


Fig. S3. XRD patterns of anatase hollow sphere (AHS) and reduced samples (AHS20, AHS40 and AHS60). High resolution XPS spectra of Ti_{2p}3/2 for AHS (a), AHS20 (b), AHS40 (c) and AHS60 (d).

The peak at 458.2 eV can be fitted into two Gaussian peaks at 458.3 and 457.9 eV , which can be assigned to Ti³⁺ and Ti⁴⁺, respectively.

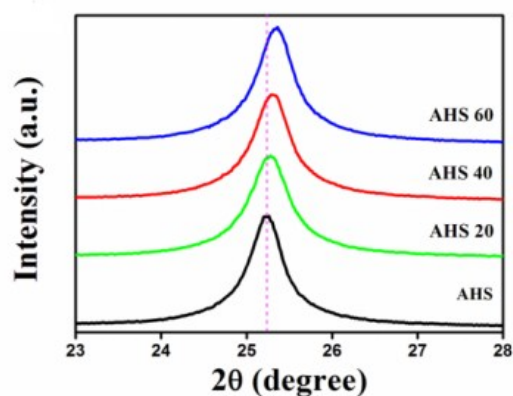


Fig. S2b Enlarged view within the 23-28° range of anatase hollow sphere (AHS) and reduced samples (AHS20, AHS40 and AHS60).

XRD patterns of all samples are illustrated in Figure S3. All of the diffraction peaks of AHS in Figure S3 correspond to the standard anatase phase of TiO_2 (JCPDS No.21-1272). After the chemical reduction treatment, all diffraction peaks of AHS20, AHS40 and AHS60 show their original phase with no additional peak. However, from the enlarge view of the 23-28° range in Fig. S2b, the (101) peak of anatase TiO_2 shifts to high-angle with a slightly broadening is observed with prolonged reaction time, which might be related to oxygen vacancies, as result of disorder-induced lattice strains and slightly reduced crystalline size.

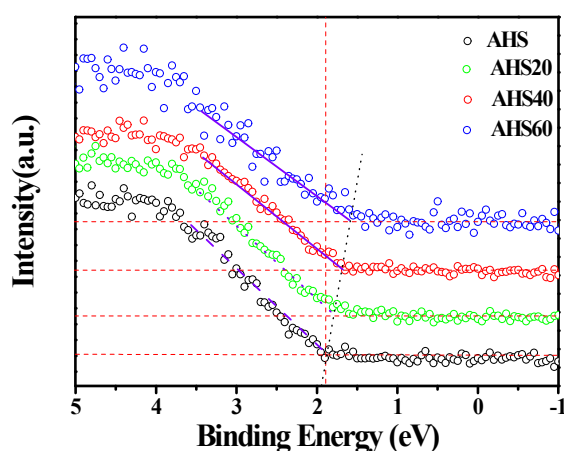


Fig. S4e. The XPS spectra of valence band of AHS, AHS20, AHS40 and AHS60.

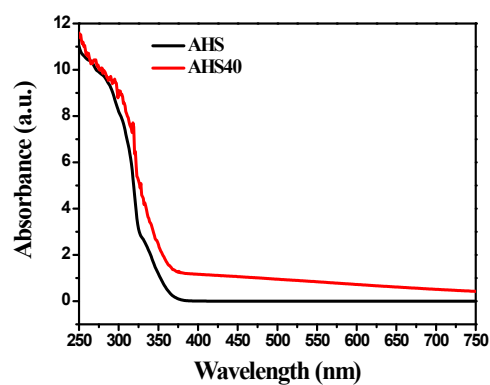


Fig. S5. The UV/Vis diffuse reflectance spectra of AHS and AHS40

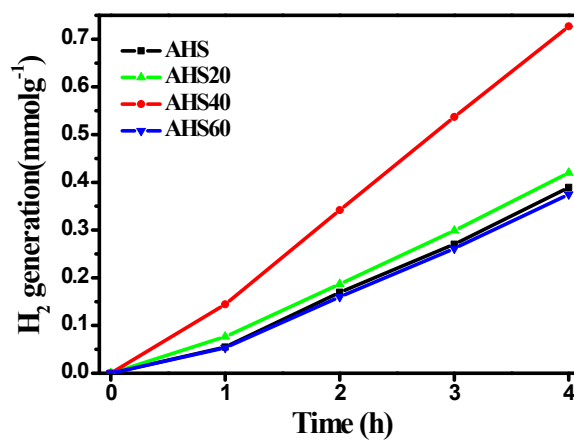


Fig. S6. Photocatalytic water splitting of AHS, AHS20, AHS40 and AHS60 under simulated sunlight.

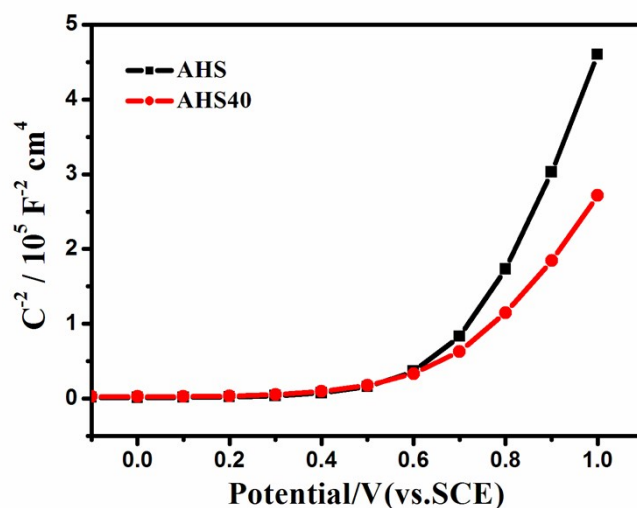


Fig. S7. Mott-Schottky plots collected at a frequency of 1 kHz in dark.

The Mott-Schottky plots of AHS and AHS40 are given in Fig. S7. Mott-Schottky plots of both samples show positive slopes characteristic of n-type semiconductors. Compared with AHS, The AHS40 showed a small slope of the Mott-Schottky plot, which implies higher charge carrier density in AHS40. The carrier density can also be calculated using the following equation:

$$N_d = \left(\frac{2}{e\epsilon\epsilon_0}\right) \left[\frac{d\left(\frac{1}{C^2}\right)}{dE}\right]^{-1}$$

Where N_d is the electron carrier density, ϵ is the dielectric constant, ϵ_0 ($F m^{-1}$) is the permittivity of vacuum, e (C) is the electron charge, $d(1/C^2)/dE$ is straight slope. The smaller slope indicating that there is the higher donor density in the AHS40.

References

- 1 S.Q. Shang, X. Jiao, and D.R. Chen, *ACS Appl. Mater. Interfaces*, 2012, **4**, 860–865
- 2 I. Tsuji, H. Kato, H. Kobayashi, A. Kudo. *J. Am. Chem. Soc.*, 2004, **126**, 13406-13413.
- 3 Z. Wang, C.Y. Yang, T.Q. Lin, H. Yin, P. Chen, D.Y. Wan, F.F. Xu, F.Q. Huang, J.H. Lin, X.M. Xie, and M.H. Jiang, *Energy Environ. Sci.*, 2013, **6**, 3007-3014.

4 M. Ye, J.J. Gong, Y.K. Lai, C.J. Lin, and Z.Q. Lin, *J. Am. Chem. Soc.*, 2012, **134**, 15720-15723.